

Dune belt restoration effectiveness assessed by UAV topographic surveys (Northern Adriatic coast, Italy)

Regine Anne Faelga ^{1*}, Luigi Cantelli ¹, Sonia Silvestri ¹, Beatrice Maria Sole Giambastiani ¹

¹ Biological, Geological and Environmental Sciences Department, University of Bologna, Bologna, 40126, Italy

5

*Correspondence to: Regine Anne Faelga (regineanne.faelga@studio.unibo.it)

Abstract. Unmanned Aerial Vehicle (UAV) monitoring surveys are used to assess a dune restoration project in the protected natural area of the Bevano River mouth in the Northern Adriatic coast (Ravenna, Italy). The impacts of the installed fences to dune development are quantified in terms of sand volume and vegetation cover changes over five years by using a systematic data processing workflow based on Structure from Motion (SfM) photogrammetry and Geomorphic Change Detection (GCD) toolset applied to two drone surveys in 2016 and 2021. Accuracy assessment is performed using statistical analysis between ground-truth and model elevation data. Results show that the fence proves to be effective in promoting recovery and growth since significant sand deposition were observed along the dune foot and front – a total area of 3799 m², volume of 1109 m³, and average depositional depth of 0.29 m. Progradation of around 3–5 m of the foredune and embryo development were also evident. There was a decrease in blowout features of about 155 m² due to increased deposition and vegetation colonization. There was also an average percent increase of 160% on wave-induced driftwood/ debris along the beach and 9.6% vegetation within the fence based on the cover analysis on selected transects. Erosion of around 1439 m² is apparent mostly at the northern portion of the structure, which could be accounted for by the aerodynamic and morphodynamic conditions around the fence and its efficiency and configuration to trap sediments. Overall, dune fencing coupled with limiting debris cleaning along the protected coast were effective. The proposed workflow can aid in creating transferable guidelines to stakeholders in ICZM implementation in the Mediterranean low-lying sandy coasts.

1. Introduction

Coastal dunes are significant ecosystems that can provide flood protection, groundwater storage, salinization prevention, species habitat, and recreation. Their dynamics are driven by the complex interaction between the controlling winds, vegetation, and the nearshore-beach geomorphology (Sloss et al., 2012; Lalimi et al., 2017). The highly dynamic nature, in addition to climatic and anthropogenic pressures, make these landforms extremely vulnerable. To prevent further degradation, soft or limited engineering, along with Nature-Based Solutions (NBS) have been the preferred intervention strategies for coastal zones as they enable a more dynamic evolution and functioning. In Europe, coastal foredunes have been stabilized over the past century by reprofiling, planting vegetation and dune fencing, and/or beach nourishment (Nordstrom

30 and Arens, 1998; Arens et al., 2001; Matias et al., 2005; Ruz and Anthony, 2008; De Vriend and Van Koningsveld, 2012; Laporte-Fauret et al., 2021).

Surface topography characterization using high-resolution data and remote sensing such as Terrestrial Laser Scanning (TLS), Light Detection and Ranging (LiDAR), and Unmanned Aerial Vehicle (UAV) has led to the development of quantitative methods used for coastal monitoring purposes (Kasprak et al., 2019). Among these, UAV platforms have gained more 35 traction due to affordability and user-friendly interface compared to other surveying counterparts. The advances in the use of UAV and Structure from Motion (SfM) photogrammetry have made geomorphic change monitoring and sediment budget estimations to become manageable approaches in research and practice (Wheaton et al., 2009a). SfM photogrammetry utilizes a structured acquisition of images to reconstruct 3D scene geometry and camera motion based on a new generation 40 of automated image-matching algorithms (Mancini et al., 2013). These images can be used to create point Digital Elevation Models (DEMs) to produce DEM of Difference (DoD) maps to estimate the net change in storage for morphological sediment budgets (Church and Ashmore, 1998; Wheaton et al., 2009a).

The use of UAV-SfM in monitoring seasonal coastal changes along the Emilia-Romagna Coast has been evident in the works of Taramelli et al. (2015), Scarelli et al. (2017), Fernandez-Montblanc et al. (2020), Sekovski et al. (2020), and Fabbri et al. (2021). These studies have noted that accuracy assessment of the surface and elevation models from UAV-SfM is 45 important before performing further analysis. Understanding the effect of elevation data uncertainty was also highlighted in the recent work of Duo et al. (2021), where UAV-derived data was utilized for the morphodynamics study of a scraped artificial dune beach in Comacchio using change detection. The availability of UAV-SfM tools and methods for coastal applications can be further utilized in other highly dynamic areas like the Ravenna coastline and its remaining dunes.

1.1 Study site information

50 The dunes along the Ravenna coast (Northern Adriatic Sea, Italy; Figure 2) have been subjected to degradation due to combined natural, anthropogenic, and climate-induced pressures. Ravenna is an historical city, known for its beach tourism and for having one of the largest seaports in Italy. It is part of the 130 km coastline of the Emilia-Romagna made up of flat alluvial sandy system, with gently sloping seabed of about 6 m in depth and shallow subtidal sediments from well-sorted fine to medium sand (Airoldi et al., 2016; Harley et al., 2016). The local hydrodynamic conditions include exposure to moderate 55 wave action and a microtidal regime that ranges between 30 and 80 cm between neap and spring tides (Biolchi et al., 2022). Two wind patterns characterize the region – the Bora wind from the northeast that brings shorter, but energetic waves (dominant wind), and the long-wave induced by Levante and Sirocco (prevailing winds) from the east and southeast, respectively. The wave climate and current circulation in the northern Adriatic are known to be strongly influenced by the Bora wind given the coast orientation.

60 According to the 2016 to 2020 meteo-marine data from the Hydro-Meteo-Climate Report of the Regional Agency for Prevention, Environment and Energy of the Emilia-Romagna Region (Arpae, 2020a), majority of the stronger waves (0.2 m to 4 m) are from NE and ENE (Figure 1). Waves blown from the eastern side are more frequent from 2016 to 2020 but are

relatively weaker (0.2 m to 2.5 m). The number of storm surges per year ranges from 17 to 24, with an average duration of 12.8 to 27.9 hours. Wind and wave data are recorded from the wave buoy every 30 minutes and are then archived to the 65 Arpae service database that can be web accessed through Dext3r (<https://simc.arpae.it/dext3r/>). Historical records of the storm surge characteristics from the 2007-2020 observations are summarized in Table 1.

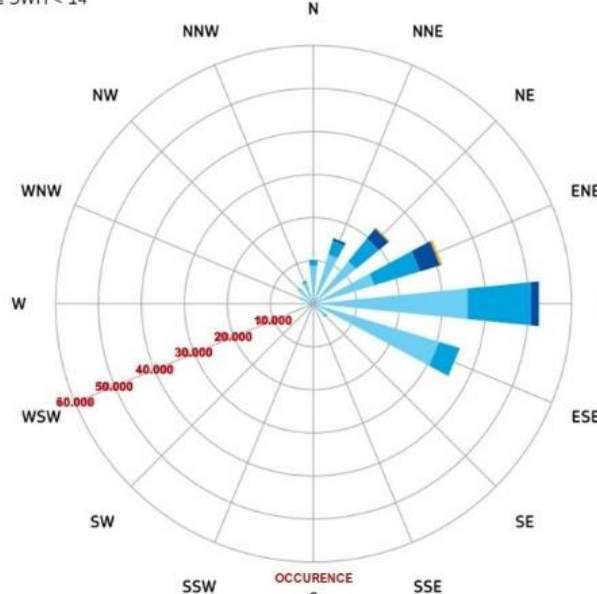
Table 1: Storm surge characteristics from 2016 to 2020 extracted from Arpae database.

Year	# of storm surge	Total duration (h)	Ave. duration (h)	Normalized energy (m ² h)	Ave. SWH (m)	Max SWH (m)	Max SL during storm surge (m)
2016	23	343	14.9	55.1	1.80	3.11	0.93
2017	17	325	19.1	95.9	1.89	3.68	0.87
2018	15	419	27.9	111.4	1.88	3.10	1.06
2019	24	307.5	12.8	41.8	1.67	2.10	1.16
2020	18	340.5	18.9	76.3	1.85	3.11	1.03

(WAVE BUOY IN CESENATICO 2007-2019)

Significant wave height (SWH, m)	Frequency
0,2 ≤ SWH < 0,5	Calm (SWH < 0,2 m): 40%
0,2 - 0,5: 34%	
0,5 ≤ SWH < 1,25	
0,5 - 1,25: 21%	
1,25 ≤ SWH < 2,5	1,25 - 2,5: 4,6%
2,5 ≤ SWH < 4	2,5 - 4: 0,64%
4 ≤ SWH < 14	4 - 14: 0%

Total data: 220.655
Valid data: 191.549
Missing data: 29.106 (13,19%)



(WAVE BUOY IN CESENATICO 2020)

Significant wave height (SWH, m)	Frequency
0,2 ≤ SWH < 0,5	Calm (SWH < 0,2 m): 40%
0,2 - 0,5: 34%	
0,5 ≤ SWH < 1,25	
1,25 ≤ SWH < 2,5	1,25 - 2,5: 4,6%
2,5 ≤ SWH < 4	2,5 - 4: 0,64%
4 ≤ SWH < 14	4 - 14: 0%

Total data: 17.567
Valid data: 17.048
Missing data: 519 (2,95%)

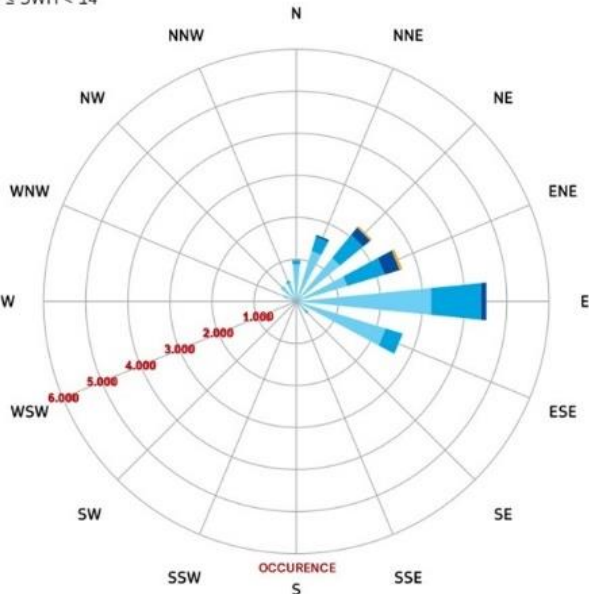


Figure 1: Significant wave height (SWH in m) and frequency (%) for 2007-2019 (a) and 2020 (b) extracted from Arpae 2020 report.

Significant land subsidence due to tectonic processes and sediment consolidation had been widespread and were intensified due to human activity since the second half of the 20th century (Airoldi et al. 2016). Erosive processes have also affected 105 km out of the 130 km coastline of the region during this period – along with the increase in vulnerability to storm surge, rapid coastal urbanization, implementation of rigid coastal defences, and massive dune destruction, igniting the need to implement strategic interventions to mitigate these problems (Arpae, 2020a). Hard coastal defences (submerged and emerged breakwaters, groynes, and revetments) were constructed in the early years (Armaroli et al., 2019; Perini et al., 2017). However, these infrastructures had negative environmental impacts including increased sedimentation of silts and clay, loss 80 of native habitats, eutrophication, and poor water quality (Airoldi et al., 2016, Preti et al., 2010; Sekovsi et al., 2020). Progressive transition from hard coastal defences in the 1970s to more integrated approaches with soft techniques and NBS in recent years were implemented in the region. NBS and soft-engineering techniques such as beach nourishment and dune fence installation have been eventually initiated as alternative solutions in early 2000. Collaborations between the regional 85 environmental agency Arpae, research groups, and other regional services that deals with coastal management led to the collection of important databases that aided the implementation of several policies to address the impending issues along the Emilia-Romagna coasts.

In 2016, the RIGED-RA Project – “Restoration and management of coastal dunes along the Ravenna coast” was able to install a grid of windbreak fences that stretches across 465 m along a portion of the Bevano River Dune Ridge in Lido di Classe (Figure 2) as an intervention strategy to reduce the vulnerability of the coast and the associated residual dunes in the 90 area (Giambastiani et al., 2016). The selection of the most suitable NBS intervention was done after a geographic, environmental, lithological, hydrogeological, geomorphological and hydrodynamical characterization of the study area collected during the three-year project. The Bevano dune–beach system is a protected natural area with high biodiversity, with laterally continuous and sub-vertical foredunes. According to Giambastiani et al. (2016), the area was selected as the 95 pilot site given that it has the potential for dune accumulation but has limited beach width and unstable sub-vertical foredune geometry. Blowouts patches are also evident along the frontal dune area of the study site. The installed fences are called ganivelles – made up of highly resistant chestnut wood stakes and poles about 1.20 m and 1.80 m in height, whose purpose is to block the wind loaded with sand and consequently favor its accumulation to recreate the dune. The spacing between stakes was set to 10 cm. First fence was placed at the dune foot followed by the second fence 2 m seawards. The two fences were connected perpendicularly by 8 m fence portions. No planting activities were implemented due to high presence of native 100 sand-binding vegetation species such as the *Psammophilous*. The fence configuration was in accordance with the mathematical model developed by Hanley et al. 2013 that illustrates the relationship between brushwood fence size, position, and optimum sand accumulation and is applicable for microtidal environments.

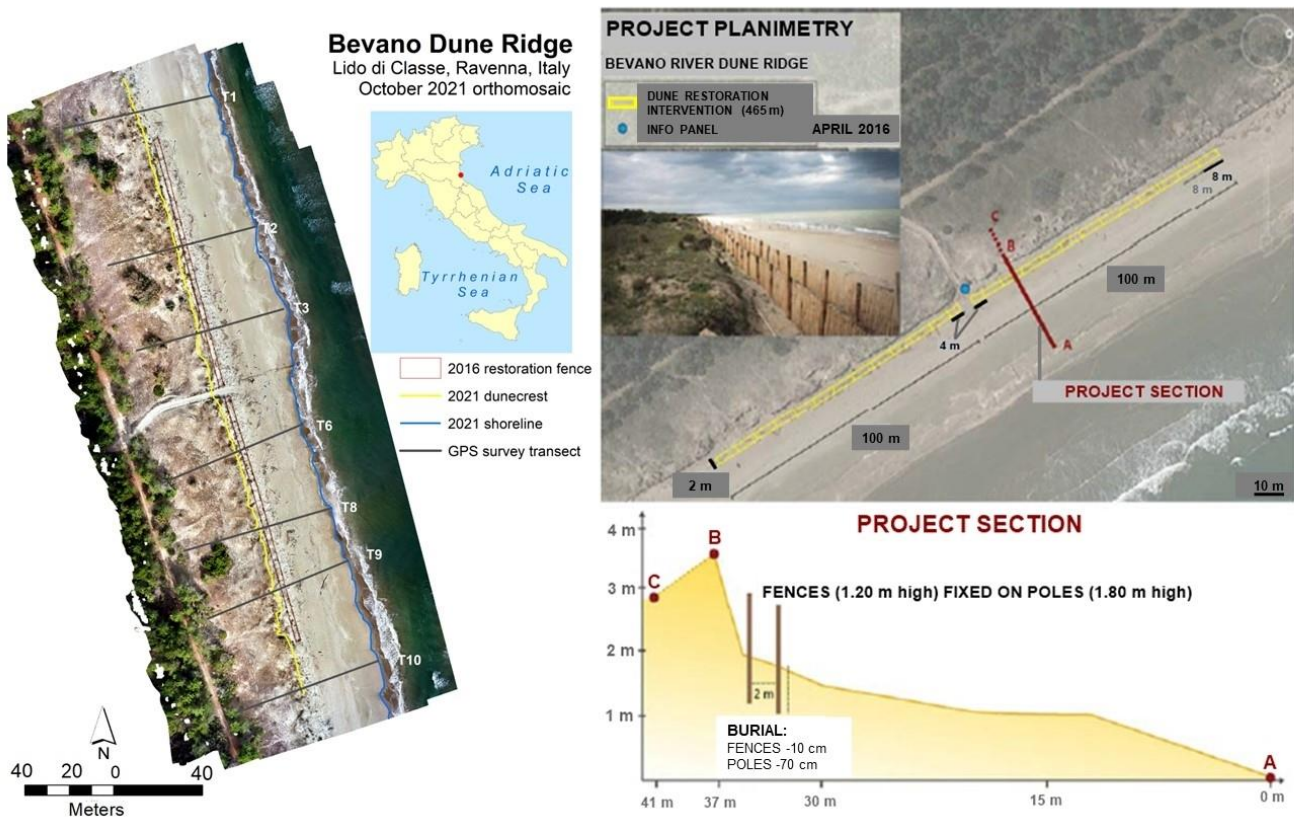


Figure 2: Location of the study area in Ravenna (Italy), and the dune fence project planimetry (modified from Giambastiani et al., 2016). Points A, B, and C represent areas in the back dune, foredune, and beach along a section of the project.

The availability of repeated UAV topographic surveys after the fence installation in 2016 and the availability of open-source tools can address the gaps in quantifying the restoration efficacy. The study aims to provide informed decision from quantitative data analysis with the proposed workflow for UAV data processing and elevation data analysis suited for sediment volume calculation. Error analysis was performed to validate the produced change detection results. Vegetation 110 cover change using orthomosaic images derived from UAV were also explored to determine other contributing factors to the overall morphology of the dune ridge.

2. Materials and Methods

The methodological framework (Figure 3) includes established workflows for data acquisition, geomorphology modelling, vegetation change, and geomorphic change detection. Annual monitoring campaigns were carried out after the fence 115 installation in 2016. In this paper, only the first (October 2016) and last (October 2021) UAV and GPS surveys were selected to assess the dune evolution. GPS data points were collected using a Leica DGPS (Viva GNSS GS15 GPS) that worked with a Real Time Kinematic (RTK) system to ensure sub metric accuracy. Collected datapoints include several profiles across the

beach from the coastline to the back dune. Aerial photographs for the 3D reconstruction were captured using a DJI Phantom drone, with flight plans defined and executed in Pix4DCapture. The flying height used in both surveys are 20 meters, with 120 side and front overlap of 80%. Ground Control Points (GCPs) were established on site and were geolocated using GPS to georeference the images and 3D models during the SfM processing in Agisoft Metashape Professional. The datum used for the flight plan was WGS 84 and the coordinate system was set to UTM 32N.

For the SfM processing, multiple overlapping photos were loaded and initial image filtering was performed before the 125 alignment process. The two datasets have a total of 13 and 15 GCPs, respectively. Each GCP was assigned as either a control or check point – the former is used to reference the model, while the latter is used to validate the camera alignment accuracy and optimization procedure results (Agisoft LLC, 2021). The 2016 data has 9 control and 4 check points while the 2021 data has 10 and 5. After the alignment process, dense point cloud was created and filtered to remove low confidence points (0-5%).

The dense point cloud were then classified into ground and non-ground using the automatic ground point classification tool 130 to remove vegetation points. The classified points were used as the boundary condition for creating the RGB orthomosaic with spatial resolution of 0.1 m x 0.1 m. Ground points were imported and converted into raster in ArcMap 10.8.2 to create the DEMs for the change detection analysis. A concurrency shapefile and spatial resolution of 0.1 m x 0.1 m was used in creating the elevation models to ensure coherence and comparability. The horizontal accuracy of the resulting DEMs was 135 assessed using the calculated Root-Mean-Square-Error (RMSE) of the check points, while the vertical accuracy was evaluated by comparing the values with the GPS profiles carried out in the field using the QGIS Profile Tool plugin version 4.2.0. Elevation values of the DEM and GPS profiles were visualized and regressed in Python 3.9. Statistical measures include R^2 , RMSE, Mean Absolute Error (MAE) and the Mean Bias Error (MBE).

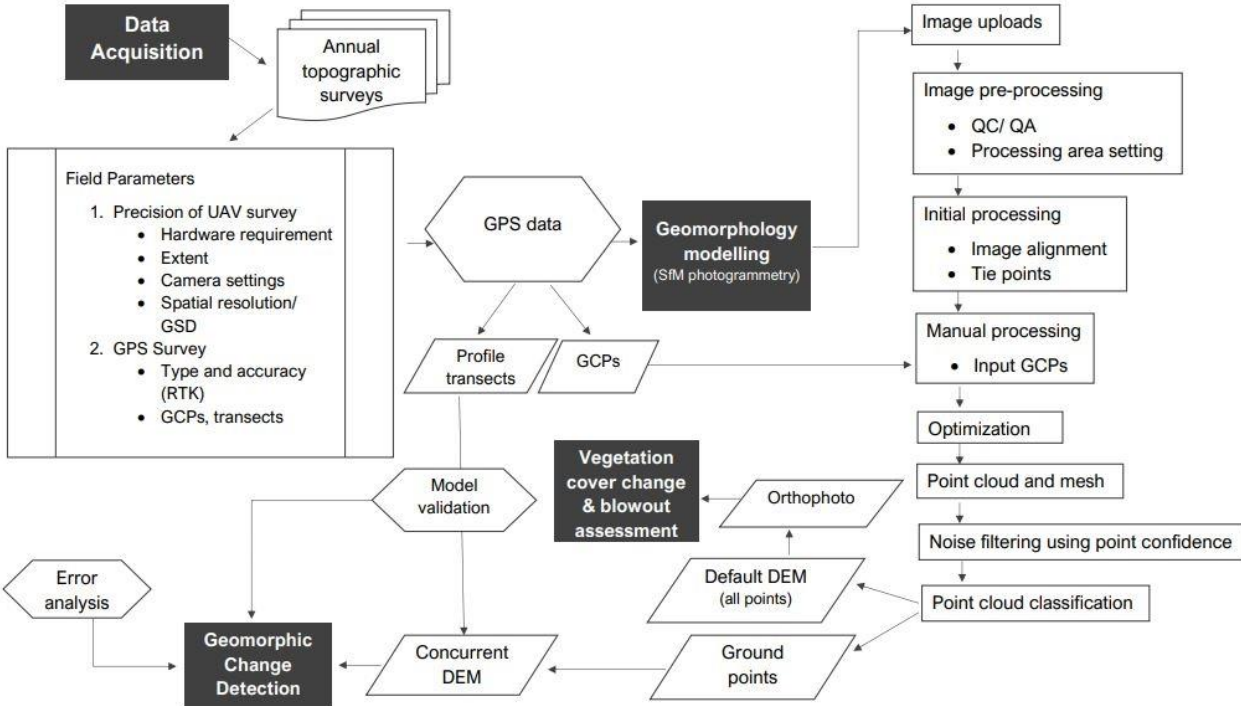


Figure 3: Methodological Framework of the study.

140 The morphological assessment was implemented using the Geomorphic Change Detection (GCD) 7 AddIn tool in ArcMap. This tool developed by Riverscapes Consortium using the methodology of Wheaton (2008), Wheaton et al. (2009a), and Wheaton et al. (2009b). It can compute for the extent, magnitude and landscape form changes that occur within an inter-survey period to understand the overall sediment budget of the area of interest (AOI) or the spatial distribution changes of sediments through time (Grams et al., 2015; Collins et al., 2016; Sankey et al., 2016). In this study, the AOI included the 145 foredune to beach area. Error rasters were created using the reported total RMSE values of the control points, which were 0.046 m and 0.032 m, respectively. These values were used to calculate the propagated error applied to each cell (Eq. 1) and the T-statistics (Eq.2) adapting the following equations from Lane et al. (2003):

$$\sigma_c = \sqrt{\sigma_1^2 + \sigma_2^2} \quad (1)$$

where σ_c is the root sum of square of uncertainty for each change interval [m]; σ_1^2 and σ_2^2 are the squares of uncertainty for 150 the older and newer time steps [m];

$$t = \frac{z_{t2} - z_{t1}}{\sigma_c} \quad (2)$$

where t is the t-statistics, z_{t2} and z_{t1} are the elevation of the raster cell for the newer (t_2) an older (t_1) time step [m]. The T-statistics can be used as a thresholding level of significant change, where values of $t > 1.96$ mean confidence interval of 95%

for a two-tailed t-test. Values that fell below the confidence threshold were removed from the output change raster to
155 improve the likelihood that a significant change was captured (Hilgendorf et al., 2021). Percent sediment imbalance metric
SI was also calculated to characterize the sediment dynamics using Equation 3 (Wheaton et al., 2013; Kasprak et al., 2015;
Kasprak et al., 2019):

$$SI = \frac{V_{DEP} - V_{EROS}}{2 * (V_{DEP} + V_{EROS})} * 100 \quad (3)$$

where V_{DEP} is the volume of deposition and V_{EROS} is the volume of erosion [m^3].

160 The vegetation change analysis was performed based on a statistical approach similar to Silvestri et al. (2022), with some
modifications applied. The process includes shoreline delineation using ISP cluster unsupervised classification in ArcMap,
transect creation based on GPS profiles, gridding and centroid creation at 1 m x 1 m resolution using the transects as
boundary conditions. The method applied to detect the presence/ absence of vegetation is based on the visual inspection of
165 the centroids of the grid cells. If the centroid falls on bare soil, there is an absence of vegetation. Consequently, if it falls on a
vegetated pixel of the photo, there is a presence of vegetation. As the orthophotos have a resolution of 0.1 m x 0.1 m, a 1 x 1
m grid resolution allows to sample one pixel (corresponding to the centroid) every 100 pixels included in each grid cell. This
method is similar to a classic visual ecological survey performed in the field with 0.1 m x 0.1 m plots placed at a distance of
170 1 m from each other along a transect, but in this case it is performed on an orthophoto instead, with the assumption that the
operator has a clear overview of the area and can clearly distinguish between vegetated and non-vegetated (either with bare
sand or logs/debris) pixels. The accuracy of the method therefore depends on the ability of the operator as well as on the
image quality. Percentage calculation of the cover types present in each transect was performed to quantify the change. The
assessment of blowout features was also performed by visual inspection of the 2016 and 2021 orthomosaic images.

3. Results

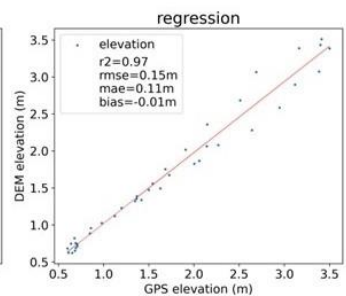
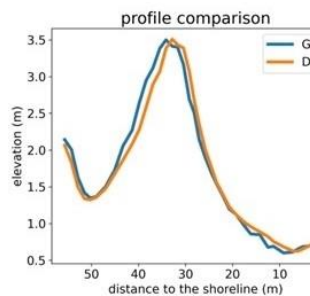
3.1. DEM development and validation

175 The DEMs, at 0.1 m x 0.1 m resolution, resulting from the UAV surveys in 2016 and 2021 are shown in Figure 4. There is
an elevation range of -0.37 to 6.30 m, with the minimum and maximum values observed along the beach area and the back
dunes. Validation on the sample transects (Figure 4b) was performed using regression analysis shown in Figure 5. Only the
2021 survey was validated for the vertical accuracy since there are no ground-truth GPS profiles available for the 2016
dataset. The R^2 values range from 0.97 to 1, while the RMSE values range from 0.07 m to 0.15 m. The MAE and error bias
180 values range from 0.06 m to 0.10 m and -0.01 m to 0.05 m, respectively. Elevation difference at the back dune area was
observed in transects 1, 3, 6, 8. There is also variation observed from the dune crest and foot in T2, 8, and 9. Overall, the
GPS data and model comparison for 2021 have good fit in all the sample profiles. In terms of horizontal accuracy, the
reported RMSE (x, y) of the 2016 and 2021 check points are 0.020 m and 0.022 m.

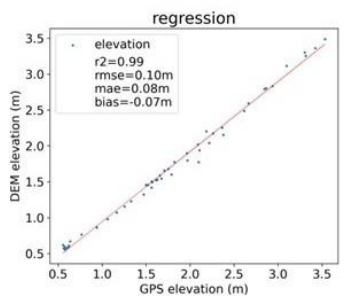
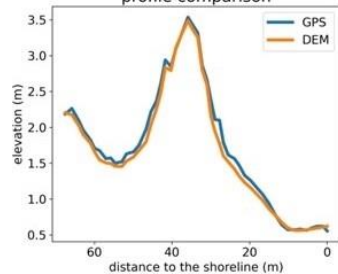


185 Figure 4: DEM of 2016 (a) and 2021 survey with GPS profiles (b).

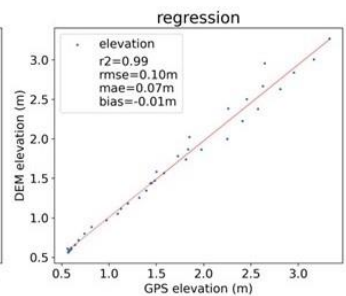
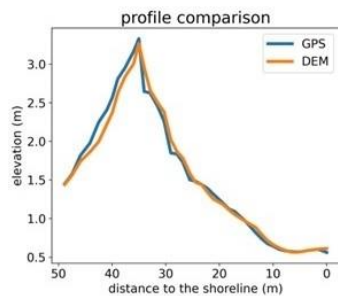
T1_2021



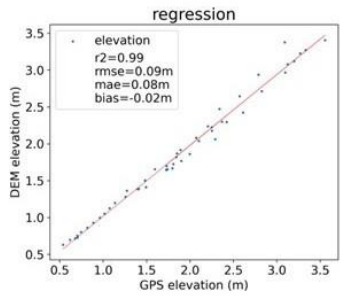
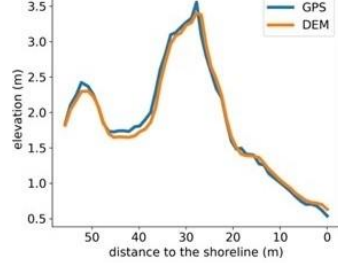
profile comparison



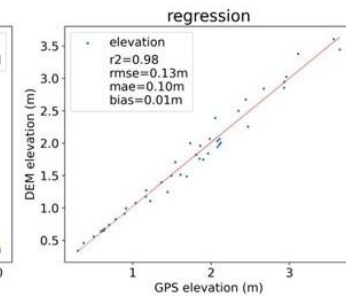
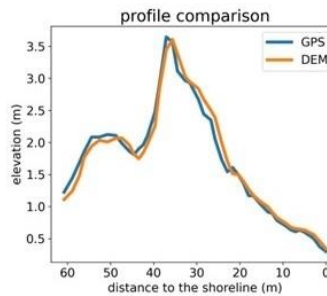
T3_2021



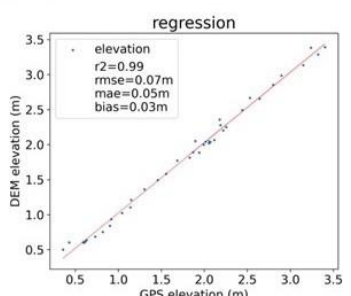
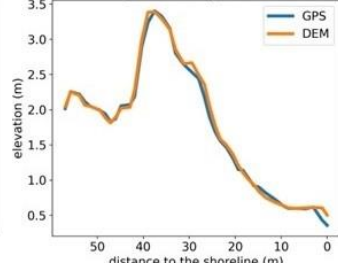
profile comparison



T8_2021



profile comparison



T10_2021

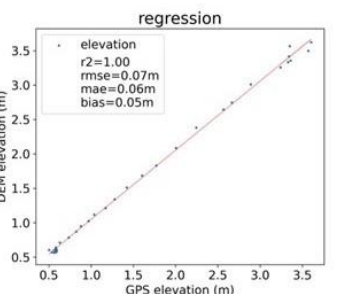
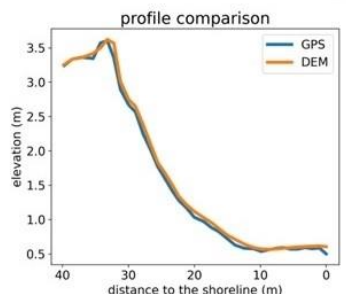


Figure 5: GPS vs DEM profile comparison for 2021.

3.2 Geomorphic and vegetation cover changes

The change detection result of the 2021 vs 2016 DEMs are shown in Figure 6 and Figure 7. Considering the total area of

190 9154 m², 6020 m² (66% of the AOI) had detectable changes after applying the 95% C.I. threshold. 2221 m² had erosional change that is equivalent to 584 m³ in volume and 0.26 m in average depth. On the other hand, 3799 m² had depositional change that corresponds to 1109 m³ and 0.29 m. A net rise of 1692 m³ has been detected, with a net volume difference of + 525 m³. The average total thickness of difference is 0.18 m, with a net thickness difference of 0.06 m. Looking at the DEM profile comparison (Figure 6b), embryo dune formation is apparent in T3, 6, 8, 9, and 10. There is also a noticeable variation 195 in elevation values in T1; but nonetheless, deposition along the dune foot is still noticeable. Overall, deposition was mostly observed within the fence and the beach at the central part of the AOI, while erosion was mostly at the northern part of the structure and at the beach part of T10. A tabular summary of the GCD is included in the Appendix.

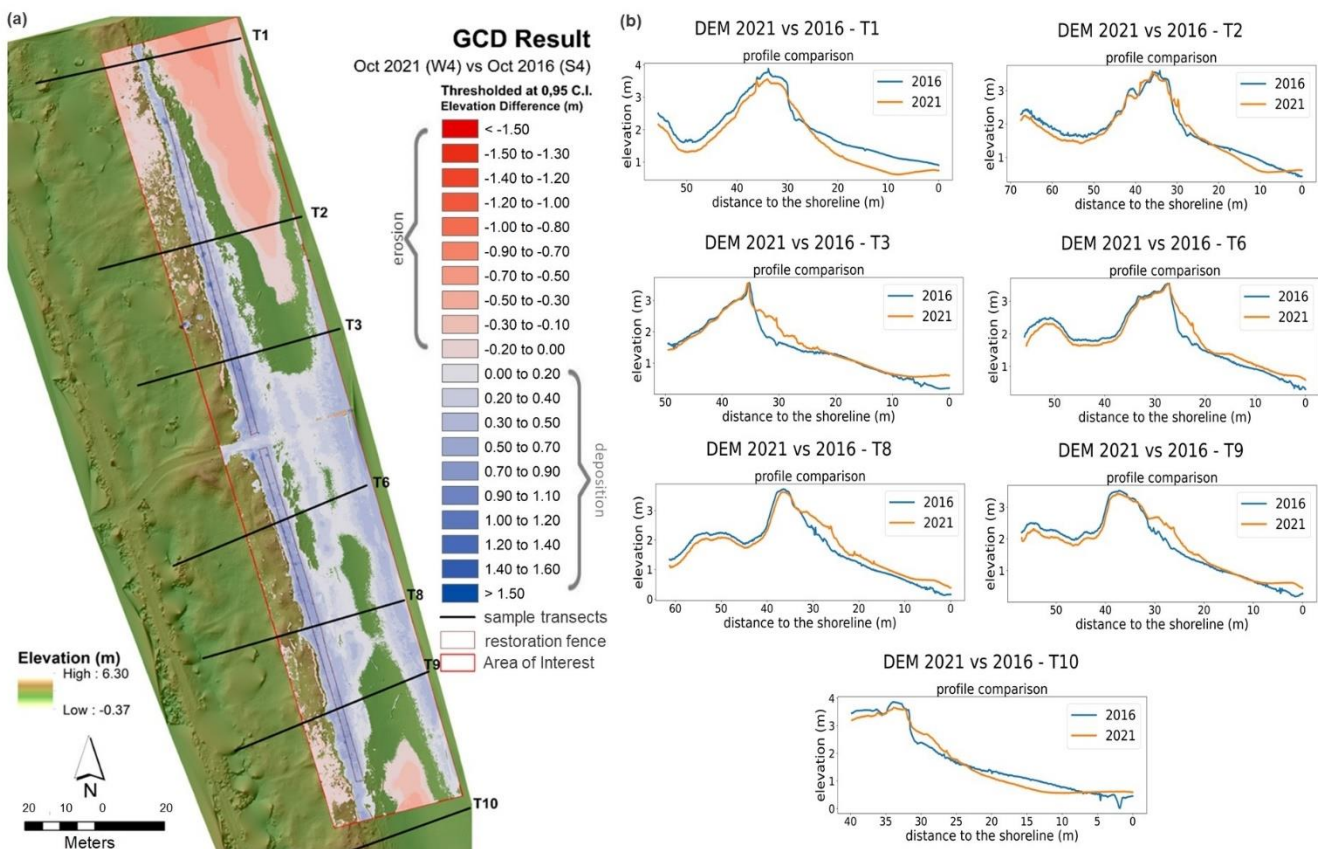


Figure 6: Change Detection result of 2021 vs 2016 DEMs (a); and DEM transect profile comparison (b).

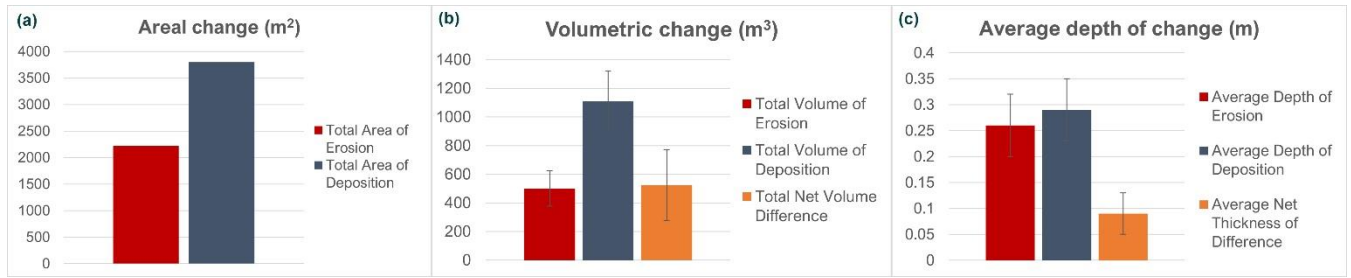
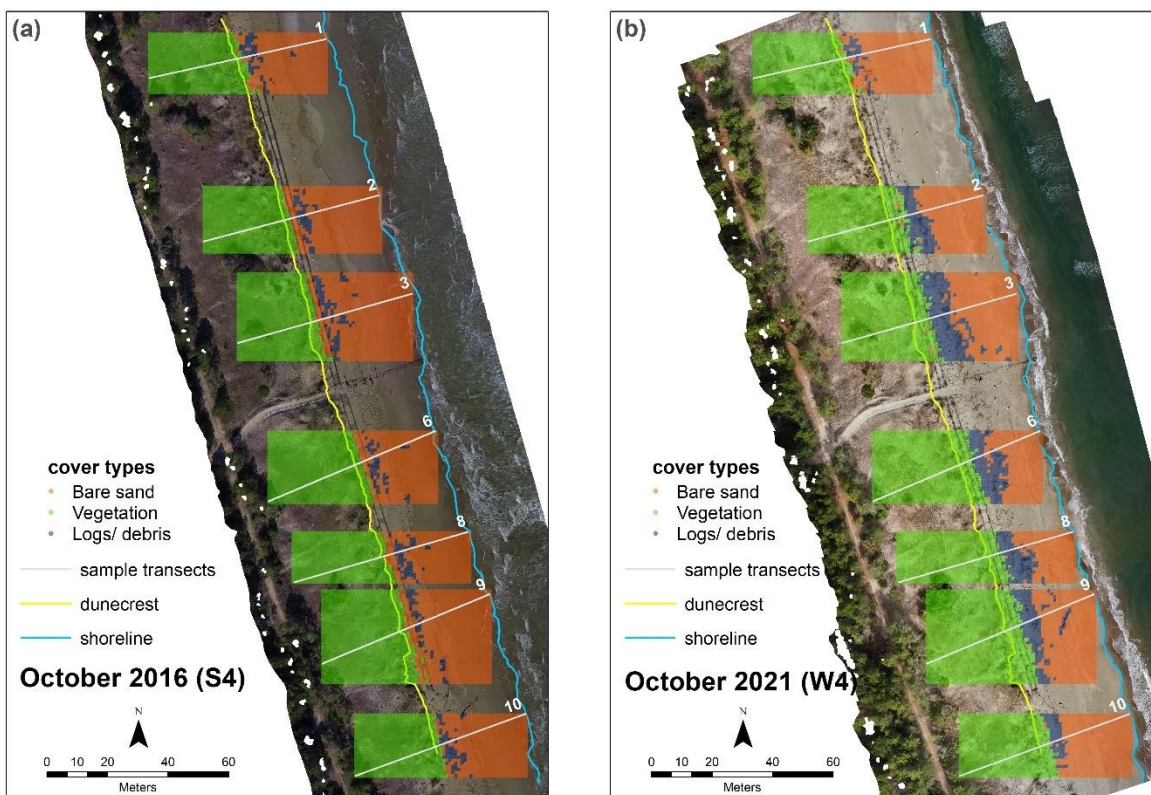
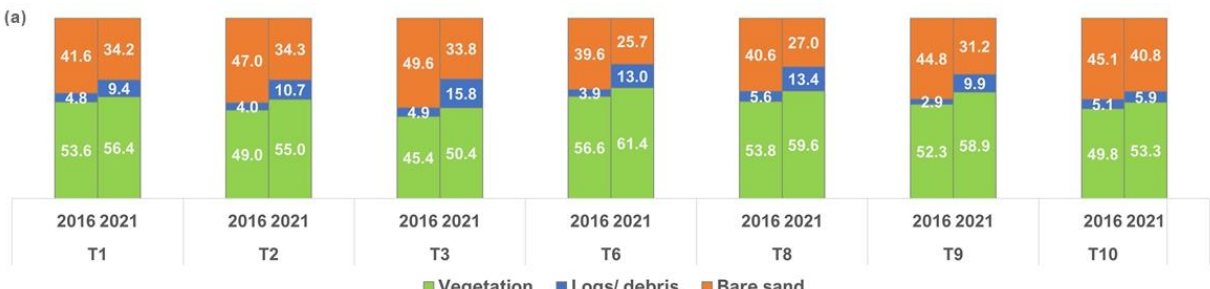


Figure 7: Summary of the areal (a), volumetric (b), and elevation changes (c).

2016 and 2021 orthomosaic images were used in the vegetation cover change assessment (Figure 8). Considering the average percent change of all the transects, there was an overall increase in the cover extent of vegetation (9.6%) and areas with logs or debris (160%) and consequently, an obvious decrease in bare sand extent (26%). The highest positive percent change for 205 vegetation increase were in T2, 3, 8, and 9. Increase in logs and debris was more evident in T2, 3, 6, 8, and 9 (Figure 9). There is also an evident decrease in blowout features on some transects located along the fence close to the dune foot, which has a total area of 155 m^2 . In Figure 10, the blowout patterns close to T2, 3, and 8 have been covered by sand and vegetation over time that is comparable to the deposition patterns in Figure 6.



210 Figure 8: Vegetation cover change maps between 2016 (a) and 2021 (b).



(b)

Transects	2016			2021			change			% change		
	Vegetation	Logs	Bare sand	Vegetation	Logs	Bare sand	Vegetation	Logs	Bare sand	Vegetation	Logs	Bare sand
T1	53.6	4.8	41.6	56.4	9.4	34.2	2.8	4.6	-7.4	5.2	94.8	-17.7
T2	49.0	4.0	47.0	55.0	10.7	34.3	6.0	6.7	-12.7	12.3	167.8	-27.1
T3	45.4	4.9	49.6	50.4	15.8	33.8	4.9	10.9	-15.8	10.9	220.7	-31.8
T6	56.6	3.9	39.6	61.4	13.0	25.7	4.8	9.1	-13.9	8.5	234.6	-35.1
T8	53.8	5.6	40.6	59.6	13.4	27.0	5.8	7.8	-13.6	10.7	139.4	-33.4
T9	52.3	2.9	44.8	58.9	9.9	31.2	6.6	7.0	-13.7	12.7	244.1	-30.5
T10	49.8	5.1	45.1	53.3	5.9	40.8	3.5	0.8	-4.3	7.0	16.3	-9.6

Figure 9: Percentage cover comparison (a) and percent change (b).



Figure 10. Sample blowout patterns observed by comparing the 2016 and 2021 orthomosaic images.

4.1 Change detection - geomorphic and vegetation cover

Within the littoral cell where the study site is located, sand accumulation and shoreline advancement by 15–20 m were observed in 2018 in comparison to the 2012 baseline data (Arpaie 2020b). The 2018 report on the coastal state of Emilia-Romagna mentioned defense intervention as one of the factors that could have influenced this change. The result of the 2021 vs 2016 GCD further establishes the efficacy of the dune fencing since significant deposition – in terms of area, average depth, and volume along the dune foot and portion of the beach was evident. Progradation of around 3 to 5 m from the foredune has been apparent and some profiles exhibit embryo development (Figure 6b, profiles 3, 6, 8, and 9). Profiles with significant deposition were the ones located at the middle and the southern part of the AOI. Embryo foredunes are formed due to sand deposition within relatively clumps of vegetation, individual plants, or driftwood/ log debris (Hesp, 2002; van Puijenbroek et al., 2017). Increase in vegetation and wave-transported driftwood have been observed within and near the fence (Figure 8). Most of the vegetation change appeared in between the fences as pioneer species colonized the pillow sand deposits. No vegetation change on the more stabilized back dune was observed. The increase in vegetation colonization has contributed to the stabilization of sand accumulation within the dunes over 5 years. The result is comparable to the study of van Puijenbroek et al. (2017) regarding the effect of vegetation on embryo dune development in the Netherlands. Tolerant vegetation facilitates sand deposition and aid in increasing stabilization and growth of dune systems (Laporte-Fauret et al., 2021; Wooton et al., 2016). The result is also in agreement with the published work of Dong et al. (2008) and Hesp (2002), where it was mentioned that the establishment of vegetation on bare sand or beach forms a roughness element that may allow localized sand deposition and reduced erosion.

An erosional pattern is apparent in the northern beach portion towards the northern head of the structure (Figure 6a), which may be accounted for by the aerodynamic and morphodynamic conditions around the dune fence, the efficiency of the fence and its configuration to trap sediments. The effects of sand trapping fences are primarily determined by its geometry, orientation relative to the main wind direction, aerodynamic roughness of the wind profile, undisturbed flow, and shelter distance (Eichmanns et al. 2021). Its influence is dependent on the given sediment boundary conditions and the wind field. In this case, the northern beach portion and the fence peripheries have relatively lesser debris and vegetation change which could have caused the erosion along the beach.

No significant increase in the foredune heights have been evident in all the profiles (Figure 6b). Similar findings have been observed in the study of Itzkin et al. (2020), where new embryo dunes are created seaward of the original dune following the emplacement of sand fences, but this has impeded the natural foredune from receiving additional sediment. Hence, dune fencing may not always be the best singular management action as it can also prevent deposition to the natural dune behind the fence that could limit vertical growth.

Human disturbances by mass tourism and coastal urbanization put detrimental impact on pioneer vegetation species and can prejudice the sustainability of foredune restoration especially in the Mediterranean (Della Bella et al., 2021). The fence has

halted human trampling on dune vegetation that had limited the formation of erosional features such as blowouts. The enforcement of limited human disturbance and the fact that it is part of a protected area had supported the restoration 250 efficacy and the spontaneous recovery of the dunes. Compared to beaches that are mechanically cleaned for recreational purposes, driftwoods that were not removed in this area acted as a form of passive restoration as well. These soft-engineering and NBS were able to induce sand accretion and vegetation colonization that can be considered as ecologically sustainable, technologically feasible, and economically viable. The fence configuration used was overall effective in trapping sediments along the dune foot and within its central bounds. However, the possibility of the fences likely to be washed away or 255 degraded over time due storm impacts should still be considered; hence, continuous monitoring and maintenance must be ensured to guarantee the long-term efficiency. Given the results, dune fencing and limiting debris cleaning can also be implemented along the other coastal zones of the Emilia-Romagna and other low-lying sandy coasts as it can aid in the sediment exchange system over time since both sediment contribution from the nearshore to the dunes and accretion rates in the foredune are vital in a beach–dune system. Sand reservoir and driftwoods within and surrounding the fence can act as 260 barriers to dissipate energy further offshore in case of major storm surge events.

4.2 Error analysis

The accuracy of the change detection model heavily depends on the quality of the input DEMs. Precision issues with the SfM-derived DEM and GPS have been encountered due to target data quality and systemic issues. The model fitting statistics of the 2021 dataset show a good fit within 0.96 to 0.99. However, a slight shift of values in the back dune is evident 265 that can be accounted to human error during the GPS survey as the pole can be dragged a few centimeters from the ground. Possible variance between in beach surfaces, systematic collection inconsistencies related to survey set-up and susceptibility to external factors, such as possible digging of the pole and wind speed influence may be encountered on beach environments surveys (Talavera et al., 2018; Casella et al., 2020; Hilgendorf et al., 2021). Misclassification of vegetation to ground points may have also affected the accuracy of the surface reconstruction of the DEMs. Drone-based topographic 270 reconstructions of beach environments tend to exhibit higher inaccuracies compared to other environments such as outcrops due to low texture and contrast of sand surface, making photogrammetric methods, such as features matching, difficult (Eltner et al., 2015; Casella et al., 2020). Another probable source of error is the lack of validation information for the vertical accuracy of the 2016 data. The GCP configurations and the number used may have also contributed to the overall model error.

275 Notwithstanding, the results show that assessing the spatio-temporal evolution of the erosional and depositional processes in the Bevano dune ridge is possible using multi-temporal drone data. Elevation model accuracy in the order of ~5 to 8 cm has been achieved. The results of the study may be further improved by ensuring consistency in camera and build parameters for the elevation and change detection models. Classifying the area of interest into geomorphic units can also be done to enhance the geomorphic change detection result.

A dune restoration project in the Northern Adriatic coast (Ravenna, Italy) was assessed using UAV monitoring surveys. SfM photogrammetry, elevation differencing, and statistical analysis were utilized to quantify dune development in terms of sand volume and vegetation cover change over time.

285 Despite the natural factors affecting the overall deposition dynamics in the area, results show that dune fencing proved to be an effective intervention to prevent dune erosion since significant geomorphological changes and vegetation colonization occurred in the 2016–2021 interval time. Main sand accumulation was observed along the dune foot where the wood fences were established. The following changes have also been observed: progradation of the front dune; development of embryo dunes; decrease of blowout features on the frontal dune area due to increase in vegetation colonization; and increase in vegetation and debris cover within and near the fences.

290 GCD can be an effective monitoring tool for coastal dunes for as long as the sources of uncertainties are considered. The results of the study can supplement in showcasing the importance of implementing dune fencing and limiting debris cleaning as nature-based solutions to prevent dune degradation along the coastal zones of the Emilia-Romagna. The proposed systematic workflow developed within this research can be transferred to other similar coastal zones and implemented into guidelines for Integrated Coastal Zone Management (ICZM).

Attribute	Raw	Thresholded DoD Estimate:	
AREAL:			
Total Area of Surface Lowering (m ²)	4,168	2,221	
Total Area of Surface Raising (m ²)	4,986	3,799	
Total Area of Detectable Change (m ²)	NA	6,020	
Total Area of Interest (m ²)	9,154	NA	
Percent of Area of Interest with Detectable Change	NA	66%	
VOLUMETRIC:			
Total Volume of Surface Lowering (m ³)	696	584 ± 124	21.32%
Total Volume of Surface Raising (m ³)	1,177	1,109 ± 213	19.20%
Total Volume of Difference (m ³)	1,873	1,692 ± 337	19.93%
Total Net Volume Difference (m ³)	481	525 ± 247	46.99%
VERTICAL AVERAGES:			
Average Depth of Surface Lowering (m)	0.17	0.26 ± 0.06	21.32%
Average Depth of Surface Raising (m)	0.24	0.29 ± 0.06	19.20%
Average Total Thickness of Difference (m) for Area of Interest	0.20	0.18 ± 0.04	19.93%
Average Net Thickness Difference (m) for Area of Interest	0.05	0.06 ± 0.03	46.99%
Average Total Thickness of Difference (m) for Area with Detectable Change	NA	0.28 ± 0.06	19.93%
Average Net Thickness Difference (m) for Area with Detectable Change	NA	0.09 ± 0.04	46.99%
PERCENTAGES (BY VOLUME)			
Percent Elevation Lowering	37%	34%	
Percent Surface Raising	63%	66%	
Percent Imbalance (departure from equilibrium)	13%	16%	
Net to Total Volume Ratio	26%	31%	

Table A1: Tabular summary of the change detection analysis.

Author contribution

Conception and study design: RAF, BMSG; Data collection: RAF, BMSG, LC; Data analysis and interpretation: RAF, BMSG, LC, SS; Article drafting: RAF; Critical revision of the article: RAF, BMSG, SS; Final approval of the version to be published: BMSG, SS, LC.

Competing interests

Some authors are members of the editorial board of the current special issue “Monitoring coastal wetlands and the seashore with a multi-sensor approach”. The peer-review process was guided by an independent editor, and the authors have also no other competing interests to declare.

Acknowledgements

Regine Anne Faelga and the collaboration among the authors were supported by the European Commission under the Erasmus Mundus Joint Master Degree Programme in Water and Coastal Management [grant number 586596-EPP-1-2017-1-IT-EPPKA1-JMDMOB].

Description	
AREAL METRICS	
Total Area of Surface Lowering (m ²)	The amount of area experiencing a lowering of surface elevations
Total Area of Surface Raising (m ²)	The amount of area experiencing an increase of surface elevations
Total Area of Detectable Change (m ²)	The sum of areas experiencing detectable surface elevation changes
Total Area of Interest (m ²)	The total amount of area under analysis (including detectable and undetectable)
Percent of Area of Interest with Detectable Change	The percent of the total area of interest with detectable changes (i.e. either exceeding the minimum level of detection or with a probability greater than the confidence interval chosen by user)
VOLUMETRIC METRICS	
Total Volume of Surface Lowering (m ³)	On a cell-by-cell basis, the DoD surface lowering depth (e.g. erosion, cut or deflation) multiplied by cell area and summed
Total Volume of Surface Raising (m ³)	On a cell-by-cell basis, the DoD surface raising (e.g. deposition, fill or inflation) depth multiplied by cell area and summed
Total Volume of Difference (m ³)	The sum of lowering and raising volumes (a measure of total turnover)
Total Net Volume Difference (m ³)	The net difference of erosion and deposition volumes (i.e. deposition minus erosion)
VOLUMETRIC METRICS NORMALIZED BY AREA	
Average Depth of Surface Lowering (m)	The average depth of lowering (surface lowering volume divided by surface lowering area)
Average Depth of Surface Raising (m)	The average depth of raising (surface raising volume divided by surface raising area)
Average Total Thickness of Difference (m) for Area of Interest	The total volume of difference divided by the area of interest (a measure of total turnover thickness in the analysis area)
Average Net Thickness Difference (m) for Area of Interest	The total net volume of difference divided by the area of interest (a measure of resulting net change within the analysis area)
Average Total Thickness of Difference (m) for Area with Detectable Change	The total volume of difference divided by the total area of detectable change (a measure of total turnover thickness where there was detectable change)
Average Net Thickness Difference (m) for Area with Detectable Change	The total net volume of difference divided by the total area of detectable change (a measure of resulting net change where there was detectable change)
NORMALIZED PERCENTAGES	
Percent of Total Volume of Difference that is surface lowering	
Percent of Total Volume of Difference that is surface raising	
Percent Imbalance (departure from equilibrium)	The percent departure from a 50%-50% equilibrium lowering/raising (i.e. erosion/deposition) balance (a normalized indication of the magnitude of the net difference)
Net to Total Volume Ratio	The ratio of net volumetric change divided by total volume of change (a measure of how much the net trend explains of the total turnover)

310 **References**

Agisoft LLC. Agisoft Metashape User Manual: Professional Edition, Version 1.7, 2021.

Airoldi, L., Ponti, M., Abbiati, M.: Conservation challenges in human dominated seascapes: The harbour and coast of Ravenna, *Regional Studies in Marine Science*, Volume 8, Part 2, Pages 308-318, ISSN 2352-4855, <https://doi.org/10.1016/j.rsma.2015.11.003>, 2016.

315 Arens, S.M., Baas, A.C.W., Van Boxel, J.H., Kaleman, C.: Influence of reed stem density on foredune development, *Earth Surf. Process. Landf.* 26, 1161–1176. <https://doi.org/10.1002/esp.257>, 2001.

Armaroli, C., Duo, E., Viavattene, C.: From Hazard to Consequences: Evaluation of Direct and Indirect Impacts of Flooding Along the Emilia-Romagna Coastline, Italy, *Frontiers in Earth Science*, 7:203. <https://doi.org/10.3389/feart.2019.00203>, 2019.

320 Arpaie Emilia-Romagna.: Rapporto IdroMeteoClima Emilia-Romagna: Dati 2020, Retrieved from <https://www.arpaie.it/it/temi-ambientali/meteo/report-meteo/rapporti-annuali> on 05 May 2022, 2020.

Arpaie Emilia-Romagna: Stato del litorale Emiliano-Romagnolo al 2018 Erosione e interventi di difesa. [ISBN 978-88-87854-48-0](#), 2020b.

325 Biolchi, L.G., Unguendoli, S., Bressan, L., Giambastiani, B.M.S., Valentini, A.: Ensemble technique application to an XBeach-based coastal Early Warning System for the Northwest Adriatic Sea (Emilia-Romagna region, Italy), *Coastal Engineering*, Volume 173, 104081, ISSN 0378-3839, <https://doi.org/10.1016/j.coastaleng.2022.104081>, 2022.

Casella, E., Drechsel, J., Winter, C., Benninghoff, M., Rovere, A.: Accuracy of sand beach topography surveying by drones and photogrammetry. *Geo-Marine Letters*, 40:255-268. <https://doi.org/10.1007/s00367-020-00638-8>, 2020.

330 Church, M., & Ashmore, P.E.: Sediment transport and river morphology: a paradigm for study, *Gravel-bed Rivers in the Environment*, 345: 115-139, 1998.

Collins, B.D., Bedford, D.R., Corbett, S.C., Cronkite-Ratcliff, C., Fairley, H.C.: Relations between rainfall-runoff-induced erosion and aeolian deposition at archaeological sites in a semi-arid dam-controlled river corridor, *Earth Surf. Process. Landf.* 41, 899–917, <https://doi.org/10.1002/esp.3874>, 2016.

335 Della Bella, A., Fantinato, E., Scarton, F., Buffa, G.: Mediterranean developed coasts: what future for the foredune restoration? *Journal of Coastal Conservation*, 25: 49, <https://doi.org/10.1007/s11852-021-00838-z>, 2021.

De Vriend, H.J., Van Koningsveld, M.: Building with Nature: Thinking, Acting and Interacting Differently, *Ecoshape*, Dordrecht, The Netherlands, p. 39. ISBN 978-94-6190-957-2, 2012.

Dong, Z., Luo, W., Qian, G., & Lu, P.: Wind tunnel simulation of the three-dimensional airflow patterns around shrubs, *J. Geophys. Res.-Earth*, 113, F02016, <https://doi.org/10.1029/2007JF000880>, 2008.

340 Eichmanns, C., Lechthaler, S., Zander, W., Pérez, M.V., Blum, H., Thorenz, F., Schüttrumpf, H.: Sand Trapping Fences as a Nature-Based Solution for Coastal Protection: An International Review with a Focus on Installations in Germany. *Environments*, 8, 135. <https://doi.org/10.3390/environments8120135>, 2021.

Eltner, A., Kaiser, A., Castillo, C., Rock, G., Neugirg, F., Abellan, A.: Image-based surface reconstruction in geomorphometry – merits, limits, and developments of a promising tool for geoscientists, *Earth Surf Dyn Discuss* 1445–1508, <https://doi.org/10.5194/esurfd-3-1445-2015>, 2015.

345 Fabbri, S., Grottoli, E., Armaroli, C., Ciavola, P.: Using High-Spatial Resolution UAV-Derived Data to Evaluate Vegetation and Geomorphological Changes on a Dune Field Involved in a Restoration Endeavour, *Remote Sensing*, 13, 1987. <https://doi.org/10.3390/rs13101987>, 2021.

Fernández-Montblanc, T., Duo, E., Ciavola, P.: Dune reconstruction and revegetation as a potential measure to decrease 350 coastal erosion and flooding under extreme storm conditions, *Ocean & Coastal Management*, Volume 188, 105075, ISSN 0964-5691, <https://doi.org/10.1016/j.ocecoaman.2019.105075>, 2020.

Giambastiani, B., Greggio, N., Sistilli, F., Fabbri, S., Scarelli, F., Candiago, S., Anfossi, G., Lipparini, C., Cantelli, L., Antonellini, M., Gabbianelli, G.: RIGED-RA project – Restoration and management of Coastal Dunes in the Northern 355 Adriatic Coast, Ravenna Area – Italy, *World Multidisciplinary Earth Sciences Symposium (WMESS 2016)*, IOP Conference Series: Earth and Environmental Science 44 (2016) 052038. doi:10.1088/1755-1315/44/5/052038, 2016.

Grams, P.E., Schmidt, J.C., Wright, S.A., Topping, D.J., Melis, T.S., Rubin, D.M.: Building sandbars in the Grand Canyon. *EOS, Transactions, American Geophysical Union* 96. <https://doi.org/10.1029/2015EO030349>, 2015.

Hanley, M.E., Hoggart, S.P.G., Simmonds, D.J., Bichot, A., Colangelo, M.A., Bozzeda, F., Heurtefeux, H., Ondiviela, B., Ostrowski, R., Recio, M., Trude, R., Zawadzka-Kahlau, E., Thompson, R.C.: Shifting sands? Coastal protection by sand 360 banks, beaches and dunes. *Coastal Engineering*. 87, 136-146. ISSN 0378-3839, <https://doi.org/10.1016/j.coastaleng.2013.10.020>, 2014.

Harley, M.D., Valentini, A., Armaroli, C., Perini, L., Calabrese, L., Ciavola, P.: Can an early-warning system help minimize the impacts of coastal storms? A case study of the 2012 Halloween storm, northern Italy. *Nat. Hazards Earth Syst. Sci.* 16, 209–222. <https://doi.org/10.5194/nhess-16-209-2016>, 2016.

365 Hesp, P.: Foredunes and blowouts: initiation, geomorphology, and dynamics, *Geomorphology* 48: 245 – 268, DOI: 10.1016/S0169-555X(02)00184-8, 2002.

Hilgendorf, Z., Marvin, M.C., Turner, C., Walker, I.J.: Assessing Geomorphic Change in Restored Coastal Dune Ecosystems Using a Multi-Platform Aerial Approach. *Remote Sensing.*, 13, 354, DOI: <https://doi.org/10.3390/rs13030354>, 2021.

Itzkin, M.; Moore, L.J.; Ruggiero, P.; Hacker, S.D.: The effect of sand fencing on the morphology of natural dune systems, 370 *Geomorphology*, 352, 106995, DOI: <https://doi.org/10.1016/j.geomorph.2019.106995>, 2020.

Kasprak, A., Wheaton, J.M., Ashmore, P.E., Hensleigh, J.W., Peirce, S.: The relationship between particle travel distance and channel morphology: results from physical models of braided rivers, *J. Geophys. Res. Earth Surf.*, 120, 55–74. <https://doi.org/10.1002/2014JF003310>, 2015.

Kasprak, A., Bransky, N.D., Sankey, J.B., Caster, J., Sankey, T.T.: The effects of topographic surveying technique and data 375 resolution on the detection and interpretation of geomorphic change, *Geomorphology*, Volume 333, Pages 1-15, ISSN 0169-555X, <https://doi.org/10.1016/j.geomorph.2019.02.020>, 2019.

Lane, S. N., Westaway, R. M., & Hicks, M.: Estimation of erosion and deposition volumes in a large, gravel-bed, braided river using synoptic remote sensing. *Earth Surface Processes and Landforms*, 28, 249–271. <https://doi.org/10.1002/esp.483>, 2003.

380 Laporte-Fauret, Q., Castelle, B., Michalet, R., Marieu, V., Bujan, S., Rosebery, D.: Morphological and ecological responses of a managed coastal sand dune to experimental notches, *Science of The Total Environment*, Volume 782, 2021, 146813, ISSN 0048-9697, <https://doi.org/10.1016/j.scitotenv.2021.146813>, 2021.

Mancini, F., Dubbini, M., Gattelli, M., Stecchi, F., Fabbri, S., Gabbianelli, G.: Using Unmanned Aerial Vehicles (UAV) for High-Resolution Reconstruction of Topography: The Structure from Motion Approach on Coastal Environments, *Remote Sensing*, 5(12):6880-6898. <https://doi.org/10.3390/rs5126880>, 2013.

385 Matias, A., Ferreira, O., Mendes, I., Dias, J.A., Vila-Consejo, A.: Artificial construction of dunes in the south of Portugal, *J. Coast. Res.*, 21, 472–481, DOI: <https://doi.org/10.2112/03-0047.1>, 2005.

Nordstrom, K.F., Arens, S.M.: The role of human actions in evolution and management of foredunes in the Netherlands and New Jersey, USA. *Journal of Conservation* 4, 169–180., DOI: <https://www.jstor.org/stable/25098280>, 1998.

390 Perini, L., Calabrese, L., Luciani, P., Olivieri, M., Galassi, G., & Spada, G.: Sea-level rise along the Emilia-Romagna coast (Northern Italy) in 2100: scenarios and impacts. *Nat. Hazards Earth Syst. Sci.*, 17, 2271–2287, <https://doi.org/10.5194/nhess-17-2271-2017>, 2017.

Preti, M., & Zanuttigh, B.: Integrated beach management at Igea Marina, Italy: results of ten-years monitoring, *Coastal Engineering Proceedings*, (32), 33-33. <https://doi.org/10.9753/icce.v32.management.33>, 2011.

395 Ruz, M.H., Anthony, E.J.: Sand trapping by brushwood fences on a beach-foredune contact: The primacy of the local sediment budget, *Zeit Geo Supp.*, 52, 179–194, DOI: 10.1127/0372-8854/2008/0052S3-0179, 2008.

Sankey, J.B., Kasprak, A., & Caster, J.: Geomorphic Process from Topographic Form: Automating the Interpretation of Repeat Survey Data to Understand Sediment Connectivity for Source-Bordering Aeolian Dunefields in River Valleys, Vol. 2016., DOI: <https://doi.org/10.1002/esp.4143>, 2016.

400 Scarelli, F.M., Sistilli, F., Fabbri, S., Cantelli, L., Barboza, E.G., Gabbianelli, G.: Seasonal dune and beach monitoring using photogrammetry from UAV surveys to apply in the ICZM on the Ravenna coast (Emilia-Romagna, Italy), *Remote Sensing Applications: Society and Environment*, Volume 7, 2017, Pages 27-39, ISSN 2352-9385, <https://doi.org/10.1016/j.rsase.2017.06.003>, 2017.

Sekovski, I., Del Río, L., Armaroli, C.: Development of a coastal vulnerability index using analytical hierarchy process and application to Ravenna province (Italy), *Ocean & Coastal Management*, Volume 183, 104982, ISSN 0964-5691, <https://doi.org/10.1016/j.ocecoaman.2019.104982>, 2020.

405 Silvestri, S., Nguyen Ngoc, D., Chiapponi, E.: Comment on “Soil salinity assessment by using near-infrared channel and Vegetation Soil Salinity Index derived from Landsat 8 OLI data: a case study in the Tra Vinh Province, Mekong Delta, Vietnam” by Kim-Anh Nguyen, Yuei-An Liou, Ha-Phuong Tran, Phi-Phung Hoang and Thanh-Hung Nguyen, *Progress in Earth and Planetary Science*, 9, pp. 1 - 8, 2022. <https://dx.doi.org/10.1186/s40645-022-00490-7>

Sloss, C. R., Shepherd, M. & Hesp, P.: Coastal Dunes: Geomorphology, *Nature Education Knowledge* 3(10):2, 2012.

Talavera, L., Del Río, L., Benavente, J., Barbero, L., López-Ramírez, J.: UAS as tools for rapid detection of storm-induced morphodynamic changes at Camposoto beach, SW Spain, *International Journal of Remote Sensing*, 39:15-16, 5550-5567, DOI: 10.1080/01431161.2018.1471549, 2018.

415 Taramelli, A., Di Matteo, L., Ciaoval, P., Guadagnano, F., Tolomei, C.: Temporal evolution of patterns and processes related to subsidence of the coastal area surrounding the Bevano River mouth (Northern Adriatic) – Italy, *Ocean & Coastal Management* 108, 74e88, 2015.

Van Puijenbroek, M., Limpens, J., De Groot, A., Riksen, M., Gleichman, M., Slim, P., van Dobben, H., Berendse, F.: Embryo dune development drivers: beach morphology, growing season precipitation, and storms: *Embryo Dune*

420 Development and Climate, *Earth Surface Processes and Landforms*, DOI: 10.1002/esp.4144, 2017.

Wheaton, J.: Uncertainty in Morphological Sediment Budgeting of Rivers, Unpublished PhD Thesis, University of Southampton, Southampton, 412 pp. Retrieved from
<https://sites.google.com/a/joewheaton.org/www/Home/research/projects-1/morphological-sediment-budgeting/phdthesis> on 09 June 2022, 2008.

425 Wheaton, J., Brasington, J., Darby, S., Sear, D.: Accounting for uncertainty in DEMs from repeat topographic surveys: improved sediment budgets, *Earth Surface Processes and Landforms*, Volume 35, Issue 2 p. 136-156.
<https://doi.org/10.1002/esp.1886>, 2009a.

Wheaton, J., Brasington, J., Darby, S., Merz, J., Pasternack, G., Sear, D., Vericat, D.: Linking geomorphic changes to salmonid habitat at a scale relevant to fish. *River Research and Applications*, Volume 26, Issue 4, p. 469-486.

430 <https://doi.org/10.1002/rra.1305>, 2009b.

Wheaton, J.M., Brasington, J., Darby, S.E., Kasprak, A., Sear, D., Vericat, D.: Morphodynamic signatures of braiding mechanisms as expressed through change in sediment storage in a gravel-bed river, *J. Geophys. Res. Earth Surf.*, 118, 759–779. <https://doi.org/10.1002/jgrf.20060>, 2013.

Yousefi Lalimi, F., Silvestri, S., Moore, L.J., & Marani, M.: Coupled topographic and vegetation patterns in coastal dunes: 435 Remote sensing observations and ecomorphodynamic implications, *J. Geophys. Res. Biogeosci.*, 122, 119–130, doi:10.1002/2016JG003540, 2017.